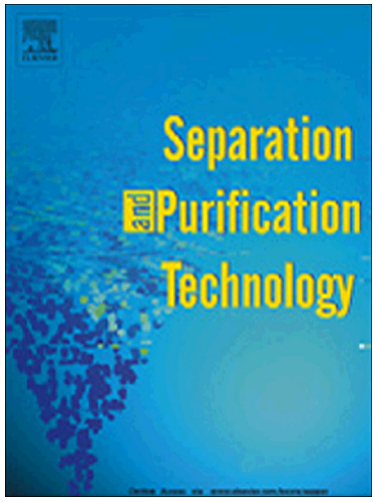

Copper ion removal from dilute solutions using ultrasonically synthesised BSA- and EWP-coated air bubbles

Amir Mohammad Nazari, Philip W. Cox, Kristian E. Waters

PII: S1383-5866(14)00311-6
DOI: http://dx.doi.org/10.1016/j.seppur.2014.05.025
Reference: SEPPUR 11772

To appear in: *Separation and Purification Technology*

Received Date: 4 April 2014
Revised Date: 12 May 2014
Accepted Date: 17 May 2014

Please cite this article as: A.M. Nazari, P.W. Cox, K.E. Waters, Copper ion removal from dilute solutions using ultrasonically synthesised BSA- and EWP-coated air bubbles, *Separation and Purification Technology* (2014), doi: http://dx.doi.org/10.1016/j.seppur.2014.05.025

Copper ion removal from dilute solutions using ultrasonically synthesised BSA- and EWP-coated air bubbles

Amir Mohammad Nazari[a], Philip W. Cox[b], Kristian E. Waters[a,*]

[a] Department of Mining and Materials Engineering, McGill University
3610 University, Montreal, Quebec, H3A 0C5, Canada
[b] School of Chemical Engineering, University of Birmingham
Edgbaston, Birmingham, B15 2TT, United Kingdom

Abstract

The aim of this study is to remove copper ions from dilute copper solution using an innovative material known as air-filled emulsion (AFE). AFE is composed of microscopic bubbles enclosed by a thin film of cysteine-rich protein distributed through the aqueous solution. The method using AEF as an extractant is combination of air-assisted solvent extraction (AASX) and biosorption techniques. The data obtained from X-ray photoelectron spectroscopy (XPS) and Fourier transform infrared (FTIR) clearly showed the thiol, amino and carboxylic groups of bovine serum albumin (BSA) and egg white protein (EWP)-coated bubbles being responsible for copper adsorption. Moreover, it was also observed that manipulation of experimental conditions such as solution pH, temperature, biosorbent and copper concentration had a significant impact on copper ion uptake. Higher solution pH led to a greater metal uptake for both egg white protein emulsion (EWPEM) and bovine serum albumin emulsion (BSAEM). At lower pH, copper removal diminished and no copper removal was obtained at pH 2 due to the high concentration of hydrogen ions. The increase of copper uptake with temperature rise was due to both the exposure of more functional groups that were initially buried in the interior of the protein structure and an increase in reaction kinetics.

Keywords: Heavy metal removal; emulsion; cysteine protein; sonochemistry; biosorption

* Corresponding author: Tel.: +1 514 398 1454. Fax: +1 514 398 4492.
Email address: Kristian.waters@mcgill.ca (K. E. Waters)

1. Introduction

Large volumes of dilute heavy metal contaminants are produced in the industrialized world including mining, metallurgical operations, steel making, petroleum, chemical manufacturing, coal and nuclear power generation (Reddad *et al.*, 2002; Deng and Ting, 2005; Masood and Malik, 2011). Heavy metals in waste have an adverse effect on the local environment due to their toxicity and accumulation in the food chain (Chen *et al.*, 2002; Sheng *et al.*, 2004; Chen and Yang, 2006; Volesky, 2007). Therefore, a series of physicochemical treatment methods such as reverse osmosis, chemical precipitation and filtration, electrochemical treatment, oxidation/reduction, evaporation and ion-exchange have been explored for heavy metal removal (Dean *et al.*, 1972; Kentish and Stevens, 2001; Reddad *et al.*, 2002). Each process has drawbacks, including high energy consumption, high operational cost, high capital cost and low selectivity (Xu and Liu, 2008; Wang *et al.*, 2009; Benaïssa and Elouchdi, 2011; Masood and Malik, 2011).

Solvent extraction (SX) is a frequently used technique in hydrometallurgical processing where the concentration of metal is relatively high (≥ 0.5 g/L) (Flett *et al.*, 1973; Ritcey and Ashbrook, 1979; Preston and Luklinska, 1980; Kentish and Stevens, 2001; Sahu *et al.*, 2004). However, long extraction times and a high solvent/aqueous ratio (~1) make this method inefficient for dilute solutions (<0.5 g/L) (Tarkan and Finch, 2005b; Li *et al.*, 2008). To overcome these challenges, several methods based on increasing the interfacial surface area between solvent and aqueous solution have been proposed, such as emulsion liquid membrane (ELM) (Valenzuela *et al.*, 2005; Sengupta *et al.*, 2006), supported liquid membrane (SLM) (Largman and Sifniades, 1978; Parthasarathy and Buffle, 1994; Kocherginsky *et al.*, 2007) and colloidal gas aphrons (CGA) (Ciriello *et al.*, 1982; Cabezo *et al.*, 1994). A novel technique known as air-assisted solvent extraction (AASX) has also been proposed to treat dilute solutions on the basis of solvent coated bubbles (Chen *et al.*, 2003; Tarkan and Finch, 2005b; 2005a). AASX exhibits promising properties such as a high specific surface area of the organic phase, high aqueous/organic ratio and excellent phase separation resulting from buoyancy effects (Tarkan and Finch, 2005b; 2005a). However, relatively low contact time between solvent-coated bubbles and metal ions, coupled with rapid disengagement of the bubbles render this method inefficient for treating large volumes of dilute solutions.

One way to boost metal ion removal from a dilute solution is through the construction of small bubbles to generate a highly stable colloidal system with well-dispersed air cells leading to an increased specific surface area, contact time and subsequently adsorption kinetics. Microbubbles (<10 μm) enclosed by a biomolecular thin film have recently received increasing attention owing to their high stability and functionality in drug delivery, micro-encapsulation of dyes and flavours, magnetic resonance imaging (MRI) and low fat foods (Avivi and Gedanken, 2005; Grinberg *et al.*, 2007; Cavalieri *et al.*, 2008; Han *et al.*, 2008a; 2008b; Grinberg *et al.*, 2009; Cavalieri *et al.*, 2010; Han *et al.*, 2010; Cavalieri *et al.*, 2011; Shchukina and Shchukin, 2011; Zhou *et al.*, 2011; Kwan and Borden, 2012). Most studies have focused on cysteine-rich protein coatings such as egg white protein (EWP), bovine serum albumin (BSA) and human serum albumin (HSA) (Avivi *et al.*, 2003; Cavalieri *et al.*, 2008; Gedanken, 2008; Vassileva and Koseva, 2010; Tchuenbou-magaia *et al.*, 2011). Cysteine-rich proteins are also capable of sorbing metals ions from wastewater streams due to the functional groups present on the surface (White *et al.*, 1956; Shindo and Brown, 1965; Mandal *et al.*, 1997; Rigo *et al.*, 2004; Dokken *et al.*, 2009; Ghosh *et al.*, 2012; Rubino and Franz, 2012). The colloidal system containing fine protein-stabilised air cells which are dispersed through the aqueous medium is termed an air-filled emulsion (AFE). AFE is generated through sonication technique. The mechanism behind protein stabilised microsphere formation is based on the combination of two steps. The first is ultrasonic emulsification including both microscopic dispersion of air cells in the aqueous solution and formation of protein clusters at the A/W interface, caused by hydrophobic interactions resulting from chemical or thermal denaturation (Suslick and Grinstaff, 1990; Grinstaff and Suslick, 1991; Zhou *et al.*, 2011). The second step is cavitation, responsible for stabilisation of microbubbles by means of formation of radicals, and subsequently disulfide crosslinking of protein molecules (Suslick and Grinstaff, 1990; Grinstaff and Suslick, 1991; Cavalieri *et al.*, 2011).

This work proposes AFE to remove copper ions from dilute solutions using EWP and BSA-coated bubbles. The effect of operational conditions such as solution pH, sorbent concentration, Cu concentration and temperature on Cu (II) adsorption qualitatively and quantitatively was explored.

2. Materials and methods

2.1. Materials

Dried chicken EWP (Sigma-Aldrich, Canada) and BSA (fraction V) (Bishop Canada Inc.) were used as supplied. All solutions were made using reverse osmosis purified water (pH of 5.8 at 25 ºC). Anhydrous cupric sulfate ($CuSO_4$) (Fisher Scientific, Canada) was used to produce the aqueous copper solution respectively. Hydrochloric acid (36%), nitric acid (67%) and hydrogen peroxide (50%) (Fisher Scientific, Canada) were used for acid digestion of the proteins. The solution pH was adjusted using 1 M sodium hydroxide (Fisher Scientific, Canada) and 1 M sulfuric acid (98%) (Fisher Scientific, Canada). 10^{-3} M KCl (Fisher Scientific, Canada) as a supporting electrolyte was utilised to measure ζ-potential of protein-coated air cells.

2.2. Emulsion preparation

5 g of protein was dissolved in 100 g of water, stirred at room temperature for a minimum of 2 hours. Insoluble particles present in EWP were removed by centrifugation (IEC Centra CL2 centrifuge, Thermo Electron Co.) (4000 rpm, 30 min, 25 ºC), while BSA particles were completely dissolved in water. The pH of the EWP solution was adjusted to 4 to reach the isoelectric point of EWP. Natural pH of BSA (7) was used to generate AFE. 80 mL of the EWP and BSA was placed in a jacketed beaker to maintain the temperature of bulk solution at 50±2 ºC and an ultrasonic horn (22 mm in diameter) was positioned at the air-protein solution interface as illustrated in Figure 1. The solution was irradiated with a high intensity sonicator (UP 400 S, 24 kHz, Hielscher Inc., U.S.A.) while compressed air was bubbled through the solution at 60 $mL.min^{-1}$ using a frit. Sonication time and power were 3 min and 90 W respectively. A second centrifugation (1000 rpm, 30 min, 25 ºC) was performed after 2 hours (to allow the dissipation of all the larger, unstable bubbles and foam) to concentrate bubbles in a top layer and separate protein debris from the EWP and BSA emulsion.

2.3. Sorption experiments

The stock copper (II) solutions were prepared by dissolving anhydrous cupric sulfate in water, and stirred for approximately 2 hours. A series of batch adsorption experiments were conducted in 50 mL centrifuge tubes to examine the effect of temperature, biomass concentration, copper concentration and pH on copper adsorption. Details of experimental condition are given in Table 1 where C_{EM} and C_{Cu} represent emulsion (BSAEM and EWPEM)

and copper concentration respectively. The required amount of BSAEM or EWPEM was added into copper solution using electronic pipette (Eppendorf Research Pro., Canada). Afterwards, the centrifuge tubes were hand shaken for 2 min to perfectly mix biosorbent and copper solution. In order to investigate the temperature effect on copper uptake, the sample temperature was controlled using a water bath. Thereafter, 15 mL of solution was withdrawn after one day followed by centrifugation (15 min, 4000 rpm) and filtration (Filter Paper No. P8, Fisher Scientific, Canada) respectively to remove BSAEM and EWPEM and also insoluble particles from the solution. In the pH effect experiment, pH of the solution was adjusted to a desired value using 1 M sulfuric acid and 1 M sodium hydroxide.

2.4. Analysis

2.4.1. Inductively coupled plasma emission spectroscopy (ICP-ES)

5 mL of supernatant after centrifugation and filtration was acid digested in two steps to remove carbon, which causes matrix interference in inductively coupled plasma emission spectroscopy (ICP-ES). Details of volumes of hydrochloric acid, nitric acid and hydrogen peroxide added to the sample given in Table 2. Sample temperature was increased to 95 ºC to increase the reaction kinetics. 1 mL of hydrogen peroxide was added to those samples which still contained precipitate after second stage. The residual copper concentration was measured by ICP-ES (Thermo Scientific 6000 series). The adsorption capacity of BSAEM and EWPEM was quantified using the percent of copper removal (R, %), calculated from the following equation:

$$R\% = \frac{(C_0 - C)}{C_0} \times 100 \quad (1)$$

Where C_0 and C are the initial and equilibrium copper concentration respectively (g/L). The equilibrium condition is achieved once there is no more change in the copper concentration in the system. The volume of protein added to the solution was taken into account in determining the initial concentration of copper ions.

2.4.2. Zeta potential measurement

ζ-potential measurements were performed on both EWPEM and BSAEM using the microelectrophoretic apparatus ZetaPlus (Brookhaven Instruments Corporation, U.S.A.). This instrument determines the electrophoretic mobility and converts to ζ-potential using Smoluchowski approximation. 10^{-3} M KCl was used instead of water to construct BSA and

EWP-coated bubbles. Afterwards, 5 ml of AFE was diluted to 30 ml using 10^{-3} M KCl. Reported values are an average of 10 measurements.

2.4.3. X-ray photoelectron spectroscopy (XPS)

XPS analysis of EWPEM and BSAEM, before and after metal ion adsorption was carried out using a monochromatic X-ray photoelectron spectrometer (Thermo Fisher scientific) to determine both the elemental composition and functional groups responsible for metal ion removal. The XPS was equipped with an Al Kα X-ray source (1486.6 eV, 0.834 nm), a microfocused monochromator, and ultrahigh vacuum chamber (10^{-9} Torr). Prior to XPS measurements, BSA and EWP powders and also precipitates of BSAEM and EWPEM obtained after copper adsorption were dried at 60 °C for 72 hours in a vacuum oven (VWR shellabs 1430). Afterwards they were finely ground using mortar and pestle. An electron flood gun was employed during XPS analysis to prevent surface charge effect. Elemental surveys from 0 to 1350 eV and high resolution were conducted with the pass energy adjusted to 1 and 0.1 eV respectively. Measurements were carried out on the three points for each sample with a spot size of 400 µm. The spectral deconvolution was performed using the software Thermo Avantage (Version 4.60).

2.4.4. Fourier transform infrared (FTIR)

In order to identify the functionalities being capable of interacting with copper ions in BSAEM and EWPEM, FTIR technique was used. The spectra were recorded using a Bruker Tensor 27 IR spectrometer within the wavenumber range of 500-4000 cm^{-1}. 1024 scans and 4 cm^{-1} resolutions were applied in collecting spectra. The background obtained from the scan of KBr was automatically subtracted from the sample spectra.

3. Results and Discussion

3.1. FTIR results

The absorbance spectra of EWP and BSA before and after copper adsorption in the range of 500-4000 cm^{-1} were recorded to clarify the nature of copper ions and protein-coated bubbles interaction. Intense characteristic bands obtained from functional groups present in biosorbent are given in Table 3. As illustrated in Figure 2, the broad and strong absorbance peaks at 3342 and 3326 cm^{-1} for both BSA and EWP are representative of amino groups (NH_2) which is consistent with the peaks at 1174 (BSA) and 1159 (EWP) attributed to C–N stretching vibration.

The bands at 2967 and 2875 cm^{-1} (BSA), 2967 and 2876 cm^{-1} (EWP) are due to asymmetric and symmetric vibration of CH_2. Strong bands at 1692 (BSA) and 1695 (EWP) cm^{-1} are attributed to the C O and C–N (amide I) stretching vibration, although amide (II) bands at 1555 (BSA) and 1568 cm^{-1} (EWP) point to C–N stretching and N–H bending respectively. The IR bands at 1445 and 1399 (BSA) cm^{-1}, 1455 and 1402 (EWP) cm^{-1} are assigned to C–H bending. The absorbance band at 1079 cm^{-1} for EWP is the result of C–O deformation, while BSA absorbance does not show any band for C–O bending. No vibrational band centered around 2550 cm^{-1} (Mandal *et al.*, 2001; Panigrahi *et al.*, 2006) was detected for S–H, as a few thiol groups are present in the structure of BSA and EWP.

Copper-loaded BSAEM illustrates that the absorbance bands at 1694, 1559 and 1456 cm^{-1} move to higher bands, while $–NH_2$ stretching, C–H asymmetric stretching of $–CH_2$, C–H bending and C–N deformation bands wave numbers are shifted to lower bands pointing to a major role of carboxylic, amide and amine groups of BSAEM in copper binding.

After copper adsorption by EWPEM, The peaks at 3326, 2967, 2876 and 1695 cm^{-1} are shifted to higher wave number; however, C–N stretching and N–H deformation absorbance band reduces to 1560 cm^{-1}. Furthermore, absorbance bands at 1455, 1402, 1159 and 1079 are disappeared. These facts indicate that carboxylic, amide and amine groups of EWPEM possibly are involved in copper adsorption.

3.2. XPS results

XPS has received much attention as a promising technique in studying the nature of chemical bond between adsorbates and adsorbents (Deng and Ting, 2005; Chen and Yang, 2006; Zheng *et al.*, 2009). In this work, XPS analysis was employed to probe the chemical interaction between functional groups present on the surface of EWP and BSA-coated bubbles and adsorbed copper ions. Figures 3A and 4A show a wide scan XPS spectrum of BSA and EWP respectively, Figure 3B and 4B, a survey scanning spectrum of Cu-loaded BSAEM and Cu-loaded EWPEM. The appearance of the Cu2p peak at a binding energy of 933.3 eV for both BSAEM and EWPEM in the XPS spectra illustrated in Figure 3B and 4B respectively is attributed to the copper accumulation on the EWP and BSA-coated bubbles.

The S2p spectral region of neat BSA and EWP illustrates a doublet peak at binding energies of 163.5-164.7 and 163.2-164.4 eV which are attributed to S–S bond. No detectable

intensity is present for thiol group which is consistent with the results obtained from FTIR. Figure 5A and 5B illustrate presence of three doublets in the sulfur spectrum. Binding energies of 161.5, 162.8 (Cu-loaded BSAEM) and 161.6, 162.6 (Cu-loaded EWPEM) indicate that the sulfur atoms are bound to the copper atoms as a thiolate species (Uvdal *et al.*, 1992; Dilimon *et al.*, 2012). The other doublet peaks are representative of disulfide and oxidized sulfur species. Due to the existence of sulfate ions (SO_4^{-2}) in the solution, an additional doublet peak at binding energies of 168, 169.3 (Cu- loaded BSAEM) and 167.9, 169.3 (Cu-loaded EWPEM) attributed to oxidized sulfur is observed (Rupp and Weser, 1976).

The Cu2p spectra of copper (Figure 6A and 6B and Table 4) illustrate the presence of CuO, Cu_2O, Cu(0), Cu–S in copper-loaded BSAEM and EWPEM which is in agreement with the mechanism of copper adsorption reported by several researchers (Atzei *et al.*, 2000; Rigo *et al.*, 2004; Dokken *et al.*, 2009; Dilimon *et al.*, 2012). Copper (II) is initially reduced to Cu (I) by RSH (a carbon-bonded to a sulfyhydryl) (Eq.1) forming an oxidized cystine (RS–SR) and then RSH reacts with Cu (I) to form the copper thiolate species (Eq. 2). It is also feasible that Cu (0) forms as a result of the reduction of Cu (I) by RSH as shown in Eq.3.

$$2CuO + 2RSH \rightarrow Cu_2O + RS–SR + H_2O \quad (1)$$

$$Cu_2O + 2RSH \rightarrow 2RSCu + H_2O \quad (2)$$

$$Cu_2O + 2RSH \rightarrow 2Cu + RS–SR + H_2O \quad (3)$$

3.3. Effect of pH

The pH impact on copper adsorption mechanism is taken into account in terms of both surface functional group of adsorbent and adsorbate solution chemistry which is based on the copper ion speciation and competition between positively charged ions (Deng and Ting, 2005; Chen and Yang, 2006). Copper exists mostly in the form of Cu^{+2} at pH below 5, however increasing the pH to above 5 results in the hydrolysis of Cu^{+2} ions and subsequently formation of $Cu(OH)^+$, $Cu(OH)_2$, $Cu(OH)_3^-$ and $Cu(OH)_4^{-2}$ in more alkaline solutions, as shown in Table 5 (Doyle and Liu, 2003). In this study, adsorption experiments were performed at a pH below 5 to prevent the occurrence of the copper speciation above.

Figure 7 details the percentage of copper adsorption onto the EWPEM and BSAEM as a function of the solution pH. No copper removal was obtained at pH 1.5 and 2 due to significantly high concentration of hydrogen ions. The positively charged hydrogen ions compete with the metal ions for binding on the ligands present on the air cells' surface, and fewer active sites are

available for the formation of copper ion complexes. Furthermore, strong electrical repulsion at lower pH for EWPEM and BSAEM prevents the metal ions from contacting the bubbles' surface. Figure 8 illustrates that the isoelectric point for both BSAEM and EWPEM is found to be at a pH between 4 and 5, indicating the presence of negatively and positively charged counter ions at the slipping planes surrounding BSA and EWP-coated bubbles respectively. In aqueous acid solution, $-COO^-$ and $-S^-$ act as the basic site and accept a proton to yield -COOH and -SH respectively. It was observed that higher pH led to greater metal uptake for both EWPEM and BSAEM, and eventually the maximum copper adsorption was obtained at pH 5, as the rise in solution pH not only decreases the hydrogen ion concentration but also increases attractive electrostatic interaction for both biosorbent. Figure 7 also indicates that EWPEM has a lower extent of copper binding compared to that observed for BSAEM. It might be due to the higher number of active binding sites present at the surface of BSA-protein coated microcells.

3.4. Temperature effect

Temperature has a noticeable effect on copper removal. As illustrated in Figure 9, copper uptake improved up to 98% and 72% assigned to BSAEM and EWPEM respectively. The increase of copper uptake with temperature rise might be due to the exposure of more functional groups that are initially buried in the interior of the protein structure (Kato *et al.*, 1981; Dickinson, 1986; Mine, 1996; Van der Plancken *et al.*, 2006). BSA and EWP exhibits a significantly compact and tight structure held together due to the presence of hydrogen bonds and covalent disulfide bridges at room temperature. Increasing the temperature to 65 °C results in the rupture of hydrogen and noncovalent bonds, unfolding the protein structure and subsequently revealing active binding sites. The other reason for higher copper removal is an increase in reaction kinetics, as temperature rise causes ions present in the solution to move faster resulting in higher probability of interaction between copper ions and functional groups on the surface of protein-coated bubbles.

3.5. Effect of biosorbent concentration

The effect of biosorbent concentration (1.5 - 25 g/L) on copper ion removal from the cupric sulfate solution at pH 5 was investigated for both EWPEM and BSAEM. As shown in Figure 10, an increase in the BSAEM concentration resulted in the higher copper removal, until maximum metal uptake was reached at a concentration of 8 g/L. Further biomass addition

diminished the copper removal and less than 5% copper uptake was observed above 20 g/L. This could be owing to the formation of bubbles aggregates at greater biosorbent dosage reducing effective surface area of bubbles and subsequently the number of functionalities for copper adsorption. Figure 10 also illustrates copper removal percentage at different EWPEM concentrations. Increasing EWPEM concentration to 25 g/L increased copper uptake due to presence of greater active sites for copper removal at higher biomass dosage. However this amount is not comparable with that of BSAEM as discussed in Section 3.3.

3.6. Effect of copper concentration

In order to investigate the effect of metal concentration on copper sorption, several experiments were carried out, shown in Figure 11 for BSAEM and EWPEM. At 0.1 g/L, maximum copper removal was obtained at BSAEM concentration of 10 g/L, however no metal uptake was seen at low copper concentrations (0.02 and 0.01 g/L). Reducing biosorbent amount to 1.2 g/L led to an increase in copper removal, up to almost 80% at Cu concentration of 0.01 g/L.

It is evident that the EWPEM is capable of binding many cupric ions at low concentration (<0.1 g/L) for specific biosorbent dosage due to the presence of more functional groups in the solution. It is interesting to note the extent of copper removal for 1.2 g/L of EWPEM is greater than that of 10 g/L. It might be an ionic strength effect that decreases in low copper concentration.

4. Conclusions

Micro-sized air cells stabilized by BSA and EWP constructed through an ultrasonic technique were used to eliminate copper ions from dilute copper solution. FTIR and XPS techniques apparently affirm that the thiol, amide, amine and carboxylate group existing on the surface of bubbles are capable of sorbing copper ion. As shown in Figure 12, copper adsorption by BSAEM and EWPEM is due to a combination of two mechanisms: Physical adsorption and complexation, where copper ions are initially attracted via electrostatic interaction; and afterwards chemical bond would be created between copper ions and functional groups. BSAEM has higher ability for copper uptake compared to that for EWPEM. It was observed that increasing both solution pH up to 5 and temperature led to higher copper adsorption. It was also

shown that the lower the biosorbent dosage, the more copper was removed at low concentration of copper ions.

Acknowledgements

The authors would like to acknowledge the financial support of Vale Base Metals and the Natural Sciences and Engineering Research Council of Canada (NSERC) for funding this project, entitled "Colloidal Solvent Extraction", through the Collaborative Research and Development Grant Program (CRDPJ–428685–11).

References

Atzei, D., Sadun, C. and Pandolfi, L., 2000. X-ray photoelectron spectra of complexes with 1-(D-3-mercapto-2-methylpropionyl)-1-proline and Ni, Cd and Cu: synthesis and LAXS study of Cu derivative. Spectrochimica Acta. Part A: Molecular and Biomolecular Spectroscopy 56(3), 531-540.

Avivi, S., Nitzan, Y., Dror, R. and Gedanken, A., 2003. An easy sonochemical route for the encapsulation of tetracycline in bovine serum albumin microspheres. Journal of the American Chemical Society 125(51), 15712-15713.

Avivi, S. and Gedanken, A., 2005. The preparation of avidin microspheres using the sonochemical method and the interaction of the microspheres with biotin. Ultrasonics Sonochemistry 12(5), 405-409.

Benaïssa, H. and Elouchdi, M.A., 2011. Biosorption of copper ions from synthetic aqueous solutions by drying bed activated sludge. Journal of Hazardous Materials 194, 69-78.

Cabezo, L.M., Caballero, M. and Perez-Bustamante, J.A., 1994. Coflotation separation for the determination of heavy metals in water using colloidal gas aphrons systems. Separation and Technology 29(11), 1491-1500.

Cavalieri, F., Ashokkumar, M., Grieser, F. and Caruso, F., 2008. Ultrasonic synthesis of stable, functional lysozyme microbubbles. Langmuir 24(18), 10078-10083.

Cavalieri, F., Zhou, M. and Ashokkumar, M., 2010. The design of multifunctional microbubbles for ultrasound image-guided cancer therapy. Current Topics in Medicinal Chemistry 10(12), 1198-1210.

Cavalieri, F., Zhou, M., Caruso, F. and Ashokkumar, M., 2011. One-pot ultrasonic synthesis of multifunctional microbubbles and microcapsules using synthetic thiolated macromolecules. Chemical Communications 47(14), 4096-4098.

Chen, F., Finch, J.A., Distin, P.A. and Gomez, C.O., 2003. Air assisted solvent extraction. Canadian Metallurgical Quarterly 42(3), 277-280.

Chen, J.P., Hong, L., Wu, S. and Wang, L., 2002. Elucidation of interactions between metal ions and Ca alginate-based ion-exchange resin by spectroscopic analysis and modeling simulation. Langmuir 18(24), 9413-9421.

Chen, J.P. and Yang, L., 2006. Study of a heavy metal biosorption onto raw and chemically modified Sargassum sp. via spectroscopic and modeling analysis. Langmuir 22(21), 8906-8914.

Ciriello, S., Barnett, S.M. and Deluise, F.J., 1982. Separation science and technology removal of heavy metals from aqueous solutions using microgas dispersions. Separation Science and Technology 17(4), 521-534.

Dean, J.G., Bosqui, F.L. and Lanouette, K.H., 1972. Removing heavy metals from wastewater. Enviromental Science & Technology 6(6), 518-522.

Deng, S. and Ting, Y-P, 2005. Characterization of PEI-modified biomass and biosorption of Cu, Pb and Ni. Water Research 39(10), 2167-2177.

Dickinson, E., 1986. Mixed proteinaceous emulsifiers: review of competitive protein adsorption and the relationship to food colloid stabilization. Food Hydrocolloids 1(1), 3-23.

Dilimon, V.S., Denayer, J., Delhalle, J. and Mekhalif, Z., 2012. Electrochemical and spectroscopic study of the self-assembling mechanism of normal and chelating alkanethiols on copper. Langmuir 28(17), 6857-6865.

Dokken, K.M., Parsons, J.G., McClure, J. and Gardea-Torresdey, J.L., 2009. Synthesis and structural analysis of copper cysteine complexes. Inorganica Chimica Acta 362(2), 395-401.

Doyle, F.M. and Liu, Z., 2003. The effect of triethylenetetraamine (Trien) on the ion flotation of Cu^{+2} and Ni^{+2}. Journal of colloid and Interface Science 258(2), 396-403.

Flett, D.S., Okuhara, D.N. and R., S.D., 1973. Solvent extraction of copper by hydroxyl oximes. Journal of Inorganic and Nuclear Chemistry 35(7), 2471-2487.

Gedanken, A., 2008. Preparation and properties of proteinaceous microspheres made sonochemically. Chemistry-A European Journal 14(13), 3840-3853.

Ghosh, S., Pandey, N.K., Bhattacharya, S., Roy, A. and Dasgupta, S., 2012. Fibrillation of hen egg white lysozyme triggers reduction of copper(II). International Journal of Biological Macromolecules 51(1), 1-6.

Grinberg, O., Hayun, M., Sredni, B. and Gedanken, A., 2007. Characterization and activity of sonochemically-prepared BSA microspheres containing Taxol-An anticancer drug. Ultrasonics Sonochemistry 14(5), 661-666.

Grinberg, O., Gedanken, A., Patra, C., Patra, S., Mukherjee, P. and Mukhopadhyay, D., 2009. Sonochemically prepared BSA microspheres containing Gemcitabine, and their potential application in renal cancer therapeutics. Acta Biomaterialia 5(8), 3031-3037.

Grinstaff, M.W. and Suslick, K.S., 1991. Air-filled proteinaceous microbubbles: synthesis of an echo-contrast agent. Proceedings of the National Academy of Sciences 88(17), 7708-7710.

Han, Y., Radziuk, D., Shchukin, D. and Moehwald, H., 2008a. Stability and size dependence of protein microspheres prepared by ultrasonication. Journal of Materials Chemistry 18(42), 5162-5166.

Han, Y., Radziuk, D., Shchukin, D. and Moehwald, H., 2008b. Sonochemical synthesis of magnetic protein container for targeted delivery. Macromolecular Rapid Communications 29(14), 1203-1207.

Han, Y., Shchukin, D., Yang, J., Simon, C., Fuchs, H. and Möhwald, H., 2010. Biocompatible protein nanocontainers for controlled drugs release. ACS Nano 4(5), 2838-2844.

Kato, A., Tsutsui, N., Matsudomi, N., Kobayashi, K. and Nakai, S., 1981. Effects of partial denaturation on surface properties of ovalbumin and lysozyme. Agricultural and Biological Chemistry 45(12), 2755-2760.

Kentish, S.E. and Stevens, G.W., 2001. Innovations in separations technology for the recycling and re-use of liquid waste streams. Chemical Engineering Journal 84(2), 149-159.

Kocherginsky, N.M., Yang, Q. and Seelam, L., 2007. Recent advances in supported liquid membrane technology. Separation and Purification Technology 53(2), 171-177.

Kwan, J.J. and Borden, M.A., 2012. Lipid monolayer collapse and microbubble stability. Advances in Colloid and Interface Science 183-184, 82-99.

Largman, T. and Sifniades, S., 1978. Recovery of copper from aqueous solutions by means of supported liquid membranes. Hydrometallurgy 3(2), 153-162.

Li, C-W, Chen, Y-M and Hsiao, S-T, 2008. Compressed air-assisted solvent extraction (CASX) for metal removal. Chemosphere 71(1), 51-58.

Mandal, S., Das, G., Singh, R., Shukla, R. and Bharadwaj, P.K., 1997. Synthesis and studies of Cu(II)-thiolato complexes: bioinorganic perspectives. Coordination Chemistry Reviews 160, 191-235.

Mandal, S., Gole, A., Lala, N., Gonnade, R., Ganvir, V. and Sastry, M., 2001. Studies on the reversible aggregation of cysteine-capped colloidal silver particles interconnected via hydrogen bonds. Langmuir 17(20), 6262-6268.

Masood, F. and Malik, A., 2011. Biosorption of metal ions from aqueous solution and tannery effluent by Bacillus sp. FM1. Journal of Environmental Science and Health. Part A, Toxic/Hazardous Substances & Environmental Engineering 46(14), 1667-1674.

Mine, Y., 1996. Effect of pH during the dry heating on the gelling properties of egg white proteins. Food Research International 29(2), 155-161.

Panigrahi, S., Kundu, S., Basu, S., Praharaj, S., Jana, S., Pande, S., Ghosh, S.K., Pal, A. and Pal, T., 2006. Cysteine Functionalized Copper Organosol: Synthesis, Characterization and Catalytic Application. Nanotechnology 17(21), 5461-5468.

Parthasarathy, N. and Buffle, J., 1994. Capabilities of supported liquid membranes for metal speciation in natural waters: application to copper speciation. Analytica Chimica Acta 284(3), 649-659.

Preston, J.S. and Luklinska, Z.B., 1980. Solvent extraction of copper(II) with ortho-hydroxyoximes—I kinetics and mechanism of extraction. Journal of Inorganic and Nuclear Chemistry 42(3), 431-439.

Reddad, Z., Gerente, C., Andres, Y. and Le Cloirec, P., 2002. Adsorption of several metal ions onto a low-cost biosorbent: kinetic and equilibrium studies. Environ Sci Technol 36(9), 2067-2073.

Rigo, A., Corazza, A., di Paolo, M.L., Rossetto, M., Ugolini, R. and Scarpa, M., 2004. Interaction of copper with cysteine: stability of cuprous complexes and catalytic role of cupric ions in anaerobic thiol oxidation. Journal of Inorganic Biochemistry 98(9), 1495-1501.

Ritcey, G.M. and Ashbrook, A.W. (1979) Solvent extraction: principles and application to process metallurgy, Amsterdam, Elsevier

Rubino, J.T. and Franz, K.J., 2012. Coordination chemistry of copper proteins: How nature handles a toxic cargo for essential function. Journal of Inorganic Biochemistry 107(1), 129-143.

Rupp, H. and Weser, U., 1976. Copper(I) and copper(II) in complexes of biochemical significance studied by X-Ray photoelectron spectroscopy. Bichimica et Biophysica Acta 446(1), 151-165.

Sahu, S.K., Agrawal, A., Pandey, B.D. and Kumar, V., 2004. Recovery of copper, nickel and cobalt from the leach liquor of a sulphide concentrate by solvent extraction. Minerals Engineering 17(7), 949-951.

Sengupta, B., Sengupta, R. and Subrahmanyam, N., 2006. Copper extraction into emulsion liquid membranes using LIX 984N-C®. Hydrometallurgy 81(1), 67-73.

Shchukina, E.M. and Shchukin, D.G., 2011. LbL coated microcapsules for delivering lipid-based drugs. Advanced Drug Delivery Reviews 63(9), 837-846.

Sheng, P.X., Ting, Y.P., Chen, J.P. and Hong, L., 2004. Sorption of lead, copper, cadmium, zinc, and nickel by marine algal biomass: characterization of biosorptive capacity and investigation of mechanisms. Journal of colloid and Interface Science 275(1), 131-141.

Shindo, H. and Brown, T.L., 1965. Infrared spectra of complexes of L-Cysteine and related compounds with zinc, Cadmium, Mercury and lead. Journal of the American Chemical Society 87(9), 1904-1908.

Suslick, K.S. and Grinstaff, M.W., 1990. Protein microencapsulation of nonaqeous liquids. Journal of the American Chemical Society 112(1), 7807-7809.

Tarkan, H.M. and Finch, J.A., 2005a. Foaming properties of solvents for use in air-assisted solvent extraction. Colloids and Surfaces A: Physicochemical Engineering Aspects 264(1), 126-132.

Tarkan, H.M. and Finch, J.A., 2005b. Air-assisted solvent extraction: towards a novel extraction process. Minerals Engineering 18(1), 83-88.

Tchuenbou-magaia, F.L., Norton, I.T. and Cox, P.W., 2011. Suspensions of air cells with cysteine-rich protein coats : Air-filled emulsions. Journal of Cellular Plastics 47(3), 217-232.

Uvdal, K., Bodo, P. and Liedberg, B., 1992. L-cysteine adsorbed on gold and copper : An X-Ray photoelectron spectroscopy study. Journal of colloid and Interface Science 149(1), 162-173.

Valenzuela, F., Fonseca, C., Basualto, C., Correa, O., Tapia, C. and Sapag, J., 2005. Removal of copper ions from a waste mine water by a liquid emulsion membrane method. Minerals Engineering 18(1), 33-40.

Van der Plancken, I., Van Loey, A. and Hendrickx, M.E., 2006. Effect of heat-treatment on the physico-chemical properties of egg white proteins: A kinetic study. Journal of Food Engineering 75(3), 316-326.

Vassileva, E.D. and Koseva, N.S. (2010) Sonochemically born proteinaceous micro- and nanocapsules, Elsevier, Advances in Protein Chemistry and Structural Biology.

Volesky, B., 2007. Biosorption and me. Water Research 41(18), 4017-4029.

Wang, X.S., Li, Z.Z. and Sun, C., 2009. A comparative study of removal of Cu(II) from aqueous solutions by locally low-cost materials: marine macroalgae and agricultural by-products. Desalination 235(1), 146-159.

White, J.M., Manning, R.A. and Li, N.C., 1956. Metal interaction with sulfur-containing amino acids. Nickel and copper complexes. Journal of the American Chemical Society 78(11), 2367-2370.

Xu, H. and Liu, Y., 2008. Mechanisms of Cd^{2+}, Cu^{2+} and Ni^{2+} biosorption by aerobic granules. Separation and Purification Technology 58(3), 400-411.

Zheng, J-C, Feng, H-M, Lam, M.H-W, Lam, P.K-S, Ding, Y-W and Yu, H-Q, 2009. Removal of Cu(II) in aqueous media by biosorption using water hyacinth roots as a biosorbent material. Journal of Hazardous Materials 171(1), 780-785.

Zhou, M., Cavalieri, F. and Ashokkumar, M., 2011. Tailoring the properties of ultrasonically synthesised microbubbles. Soft Matter 7(2), 623-630.

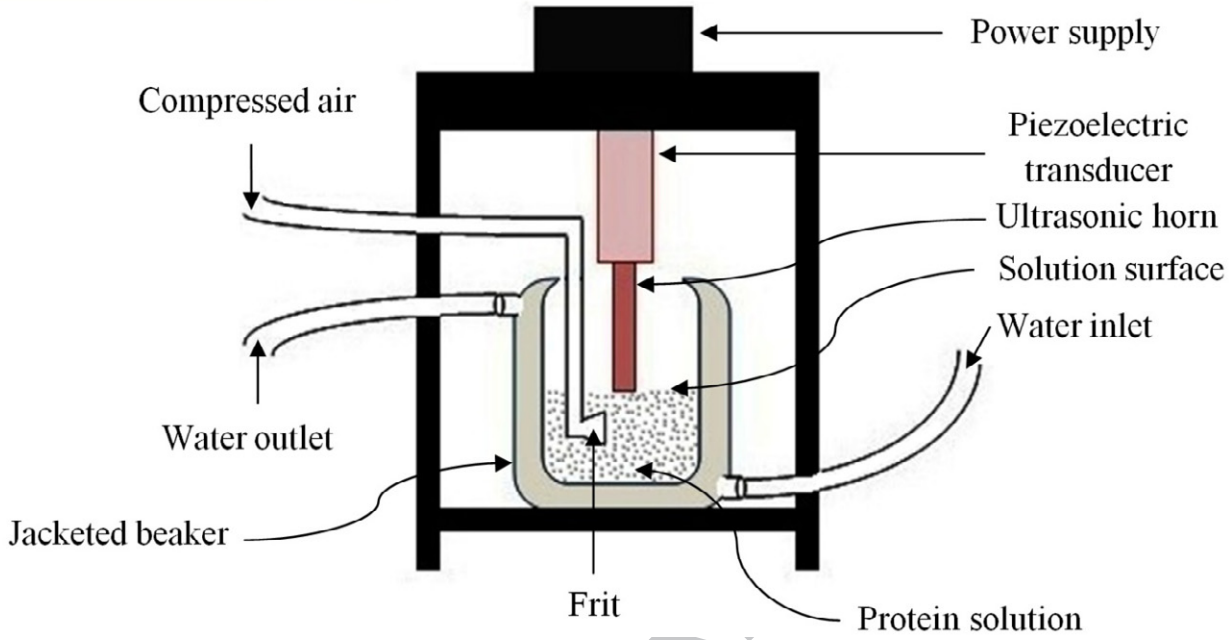

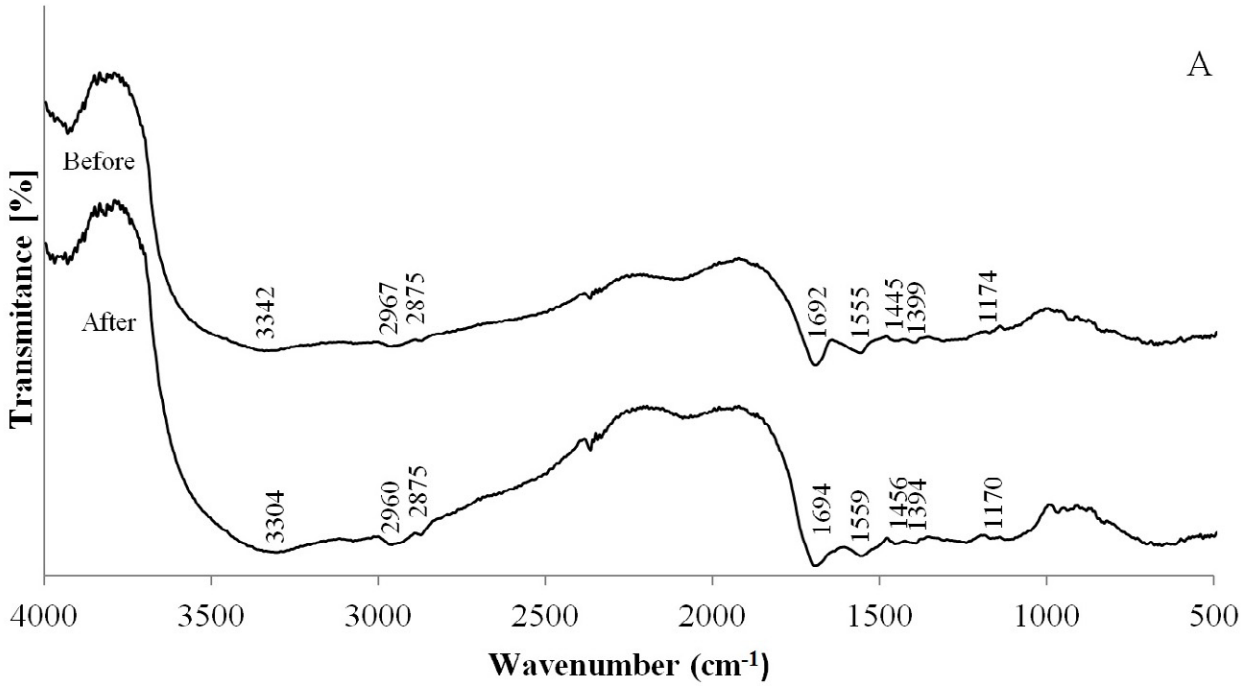
A
Before
After
Transmitance [%]
3342
2967
2875
1692
1555
1445
1399
1174
3304
2960
2875
1694
1559
1456
1394
1170
4000
3500
3000
2500
2000
1500
1000
500
Wavenumber (cm-1)

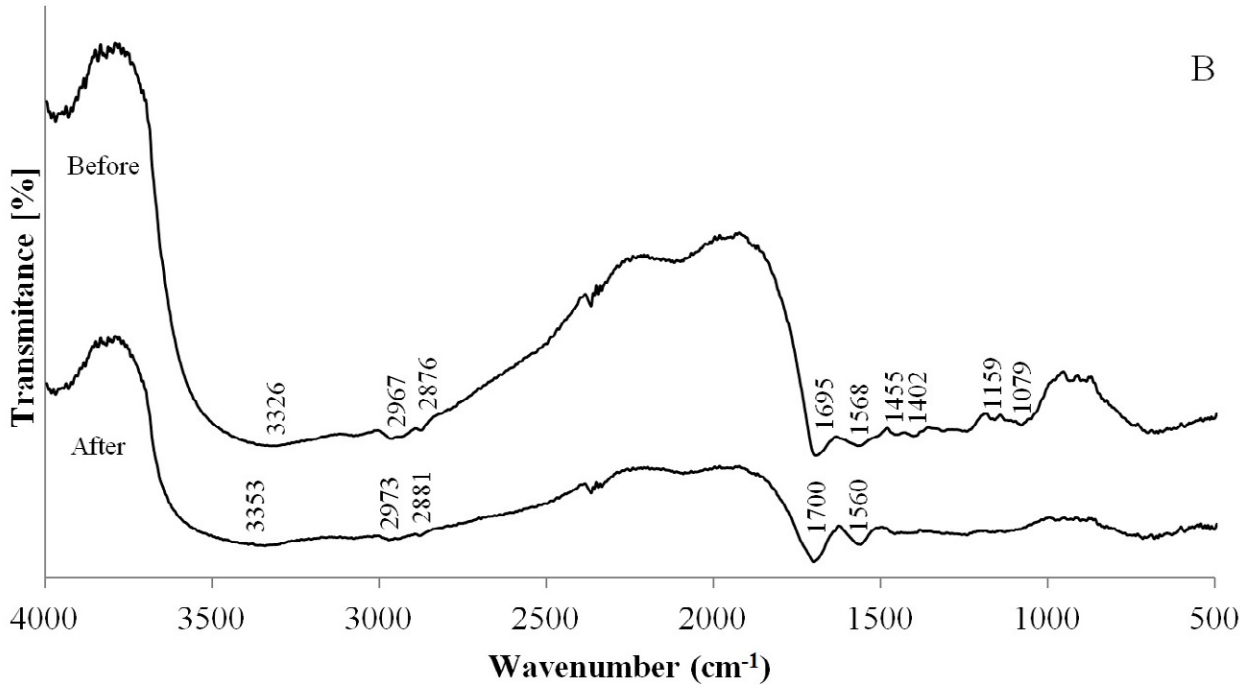
B
Before
After
Transmitance [%]
3326
2967
2876
1695
1568
1455
1402
1159
1079
3353
2973
2881
1700
1560
4000
3500
3000
2500
2000
1500
1000
500
Wavenumber (cm-1)

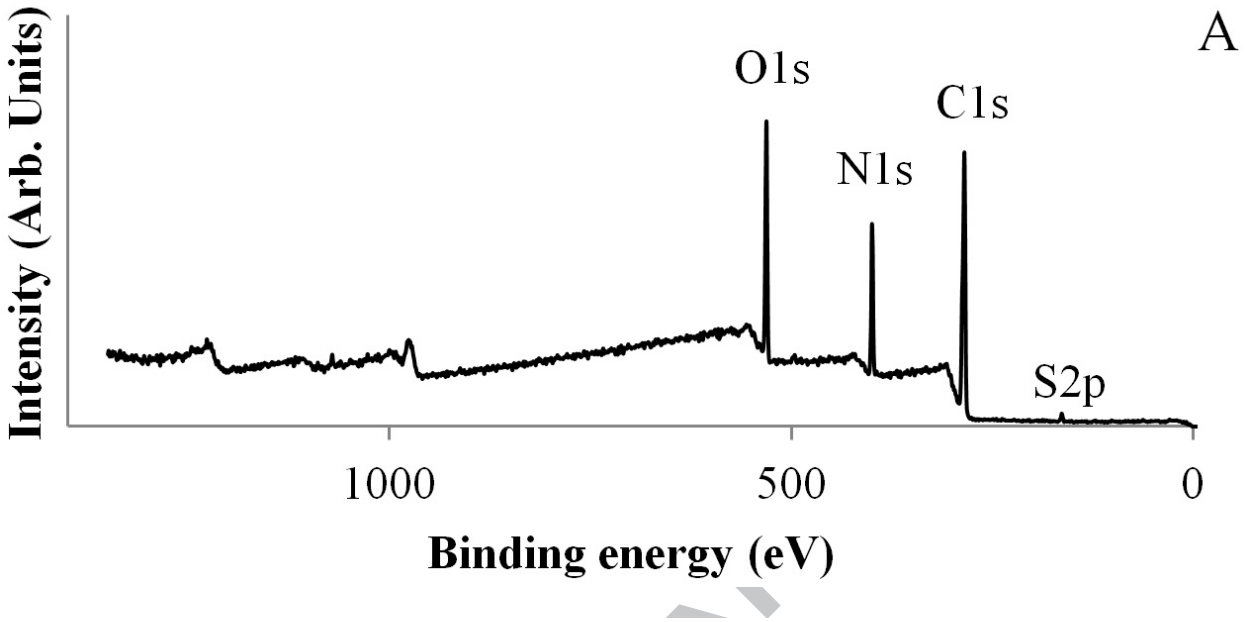
A
O1s
C1s
N1s
S2p
Intensity (Arb. Units)
1000
500
0
Binding energy (eV)

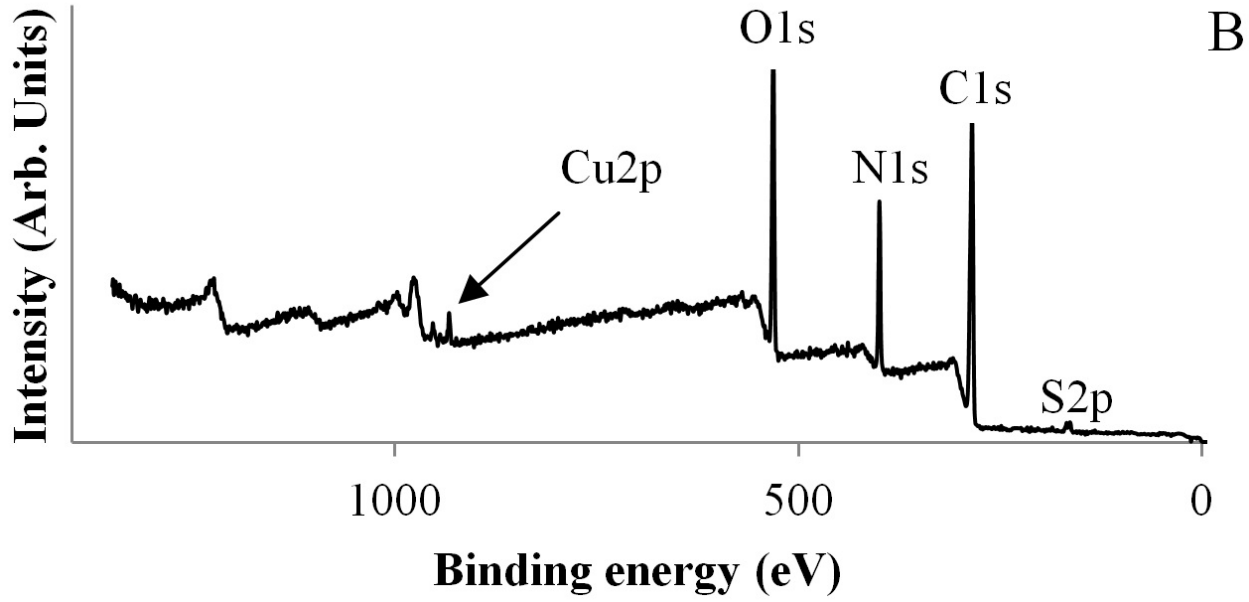
B
O1s
C1s
Cu2p
N1s
S2p
Intensity (Arb. Units)
1000
500
0
Binding energy (eV)

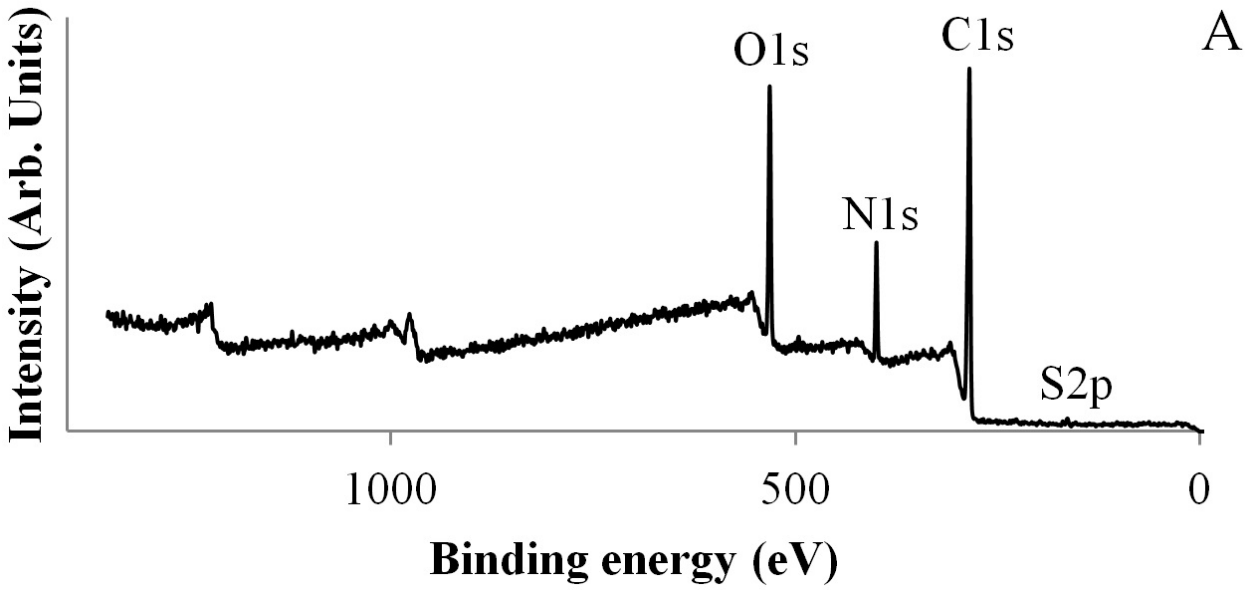
A
O1s
C1s
N1s
S2p
Intensity (Arb. Units)
1000
500
0
Binding energy (eV)

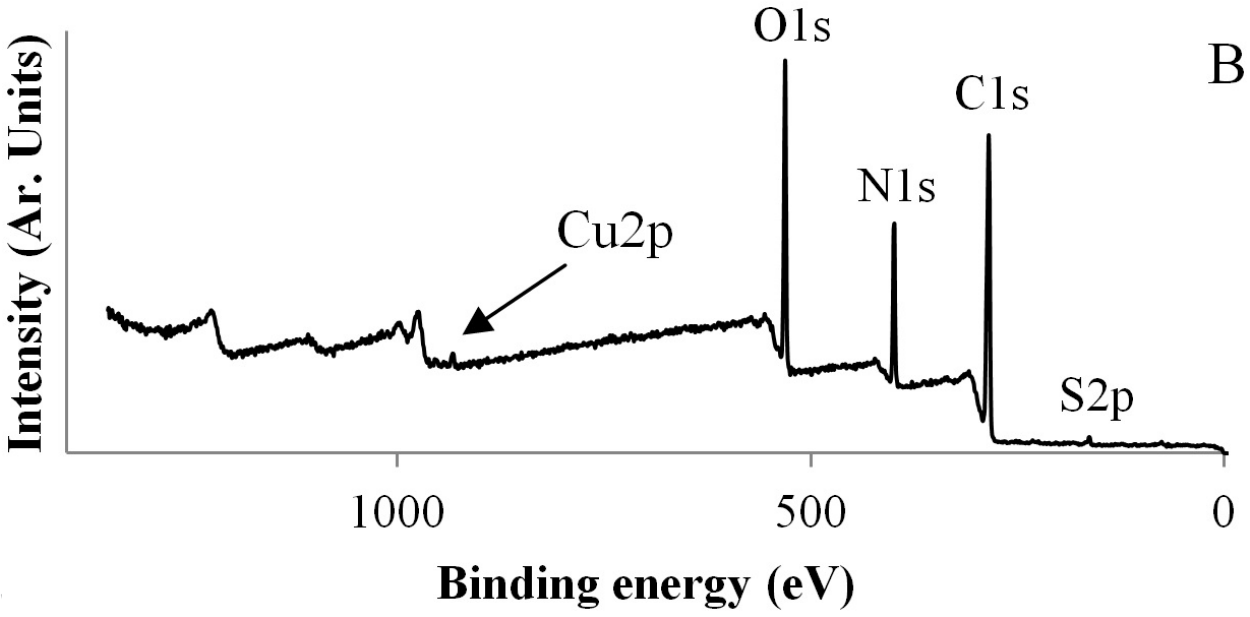
B
O1s
C1s
N1s
Cu2p
S2p
Intensity (Ar. Units)
1000
500
0
Binding energy (eV)

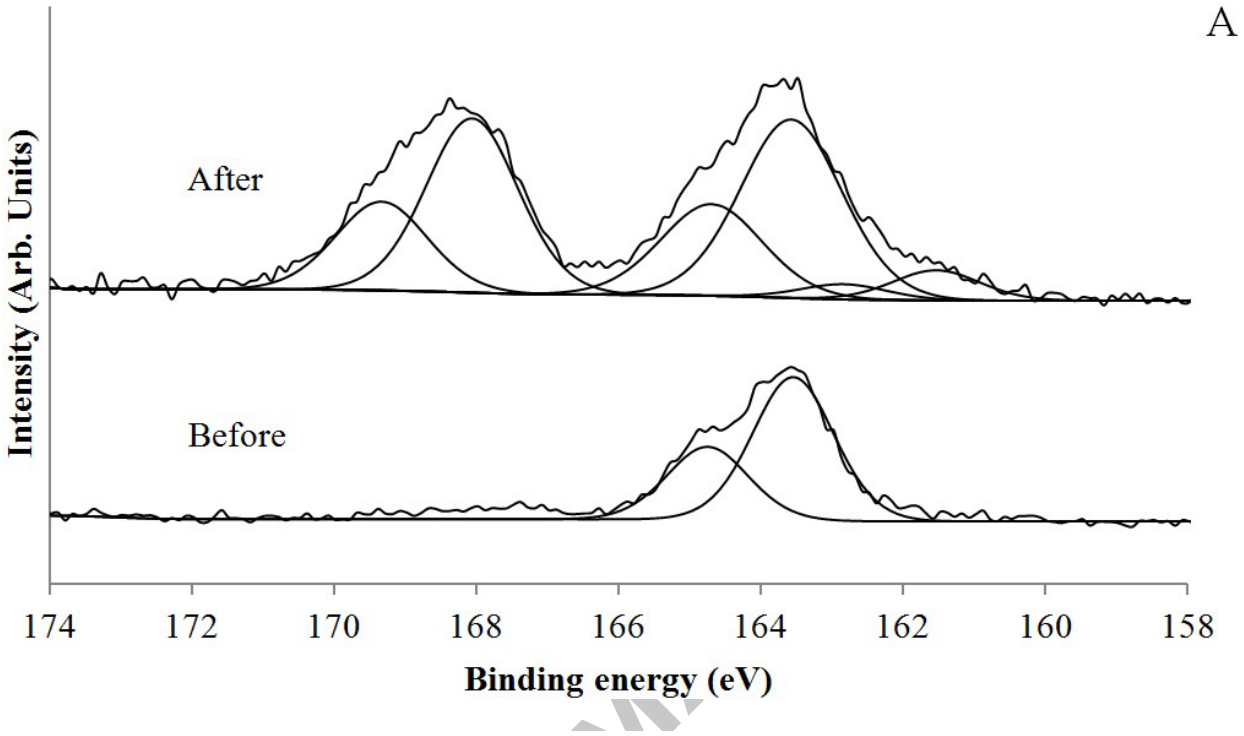
A
After
Before
Intensity (Arb. Units)
174
172
170
168
166
164
162
160
158
Binding energy (eV)

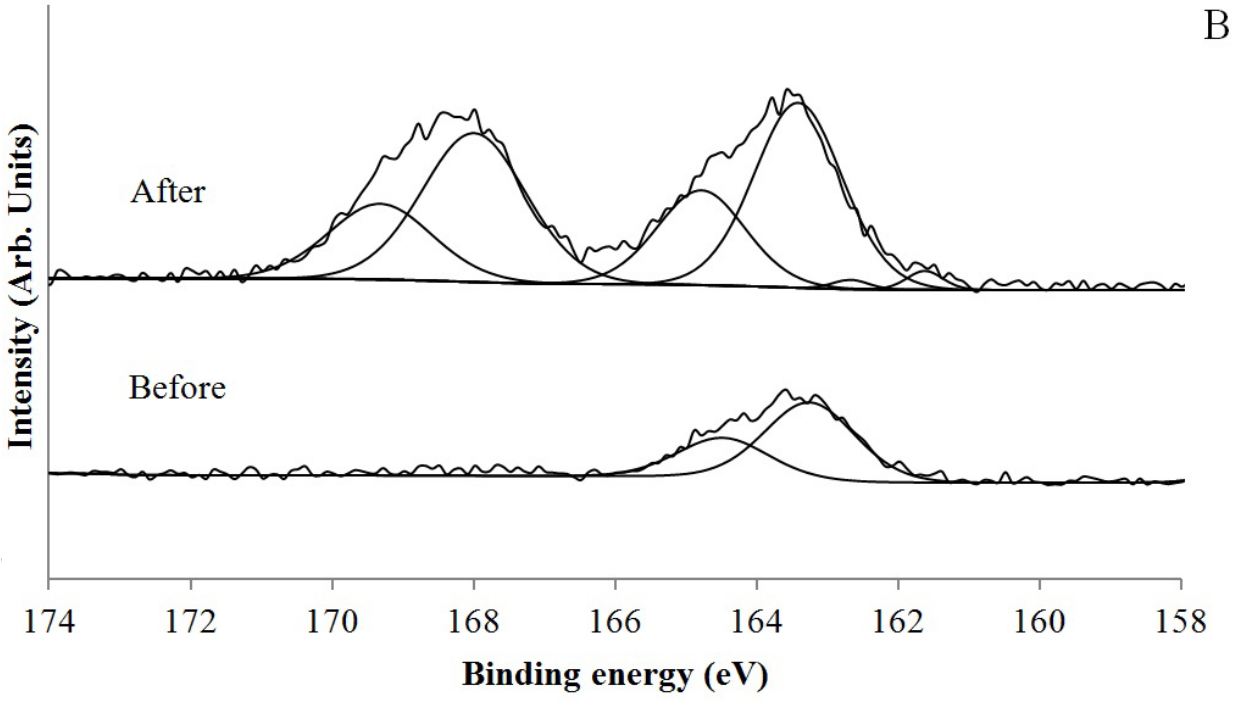
B
After
Before
Intensity (Arb. Units)
174
172
170
168
166
164
162
160
158
Binding energy (eV)

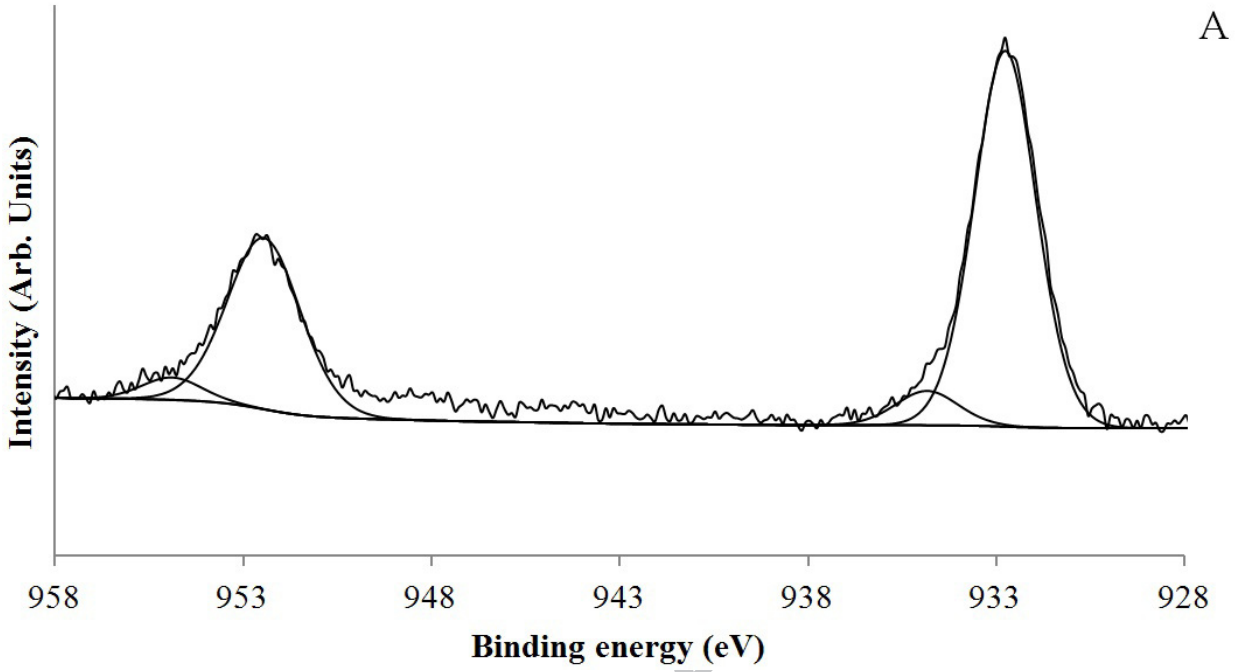
A
Intensity (Arb. Units)
958
953
948
943
938
933
928
Binding energy (eV)

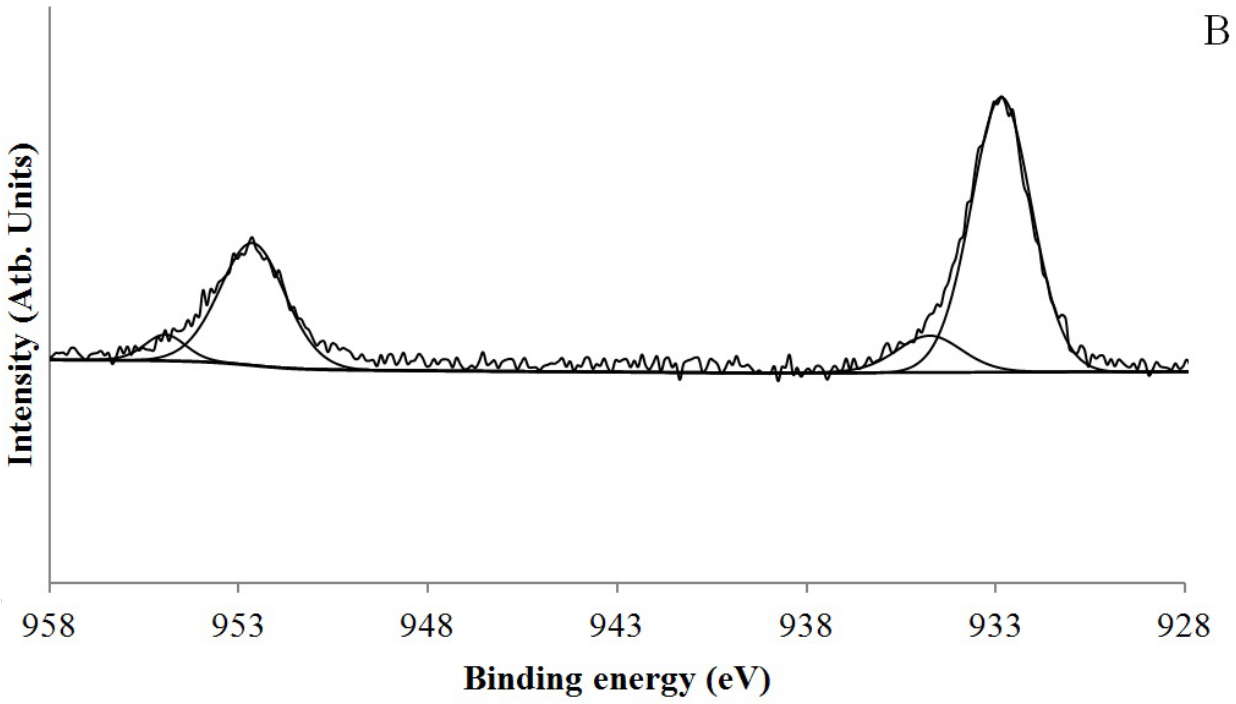
B
Intensity (Atb. Units)
958
953
948
943
938
933
928
Binding energy (eV)

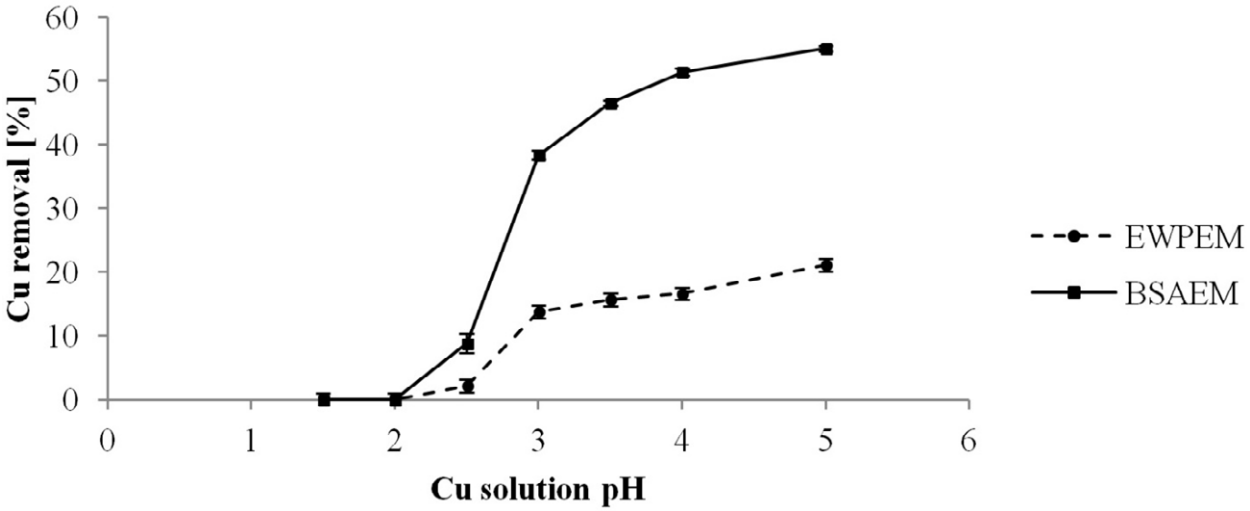

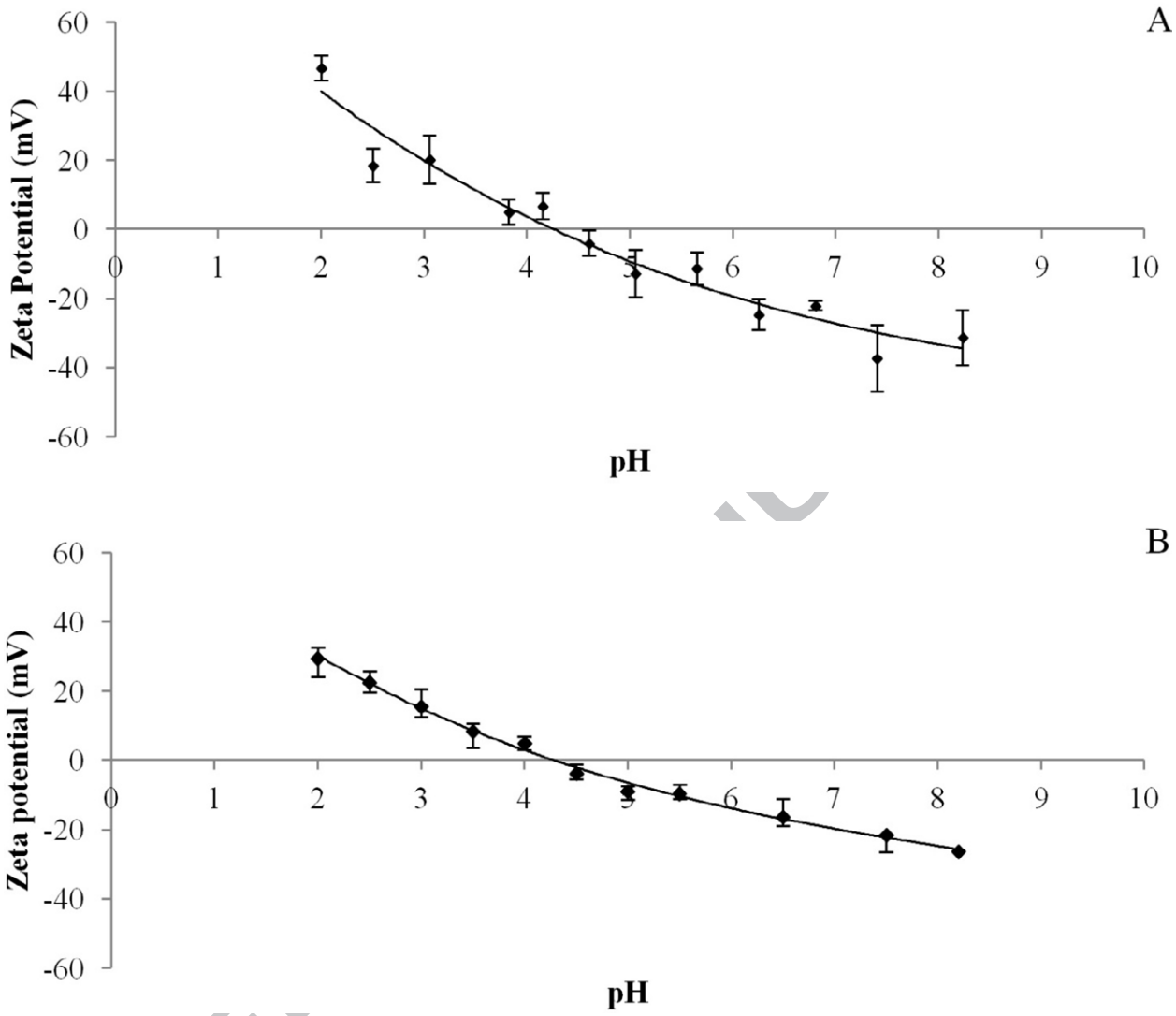
A
Zeta Potential (mV)
60
40
20
0
-20
-40
-60
0
1
2
3
4
5
6
7
8
9
10
pH
B
Zeta potential (mV)
60
40
20
0
-20
-40
-60
0
1
2
3
4
5
6
7
8
9
10
pH

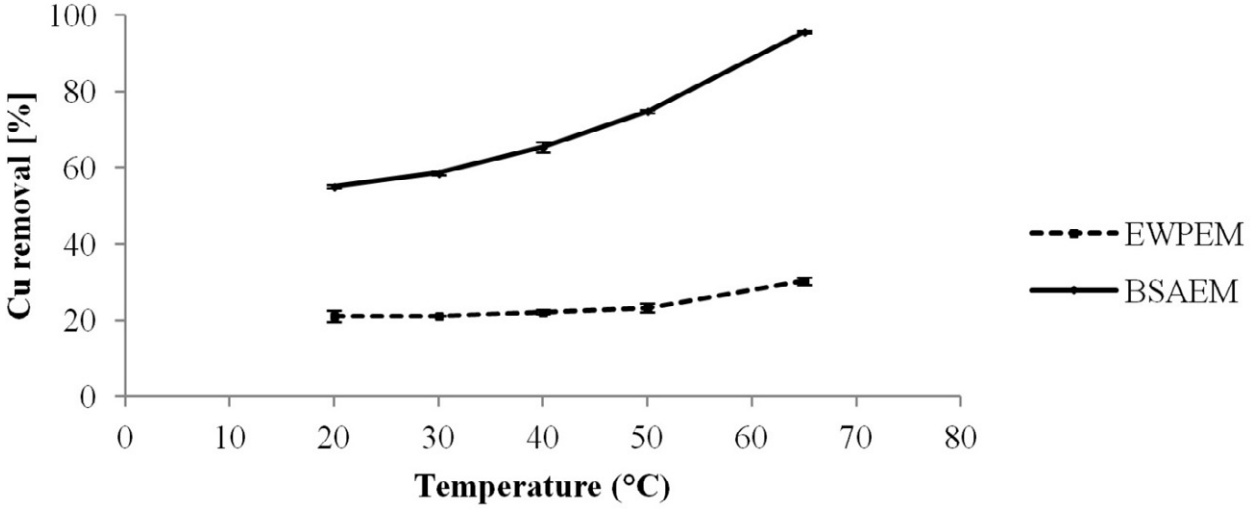

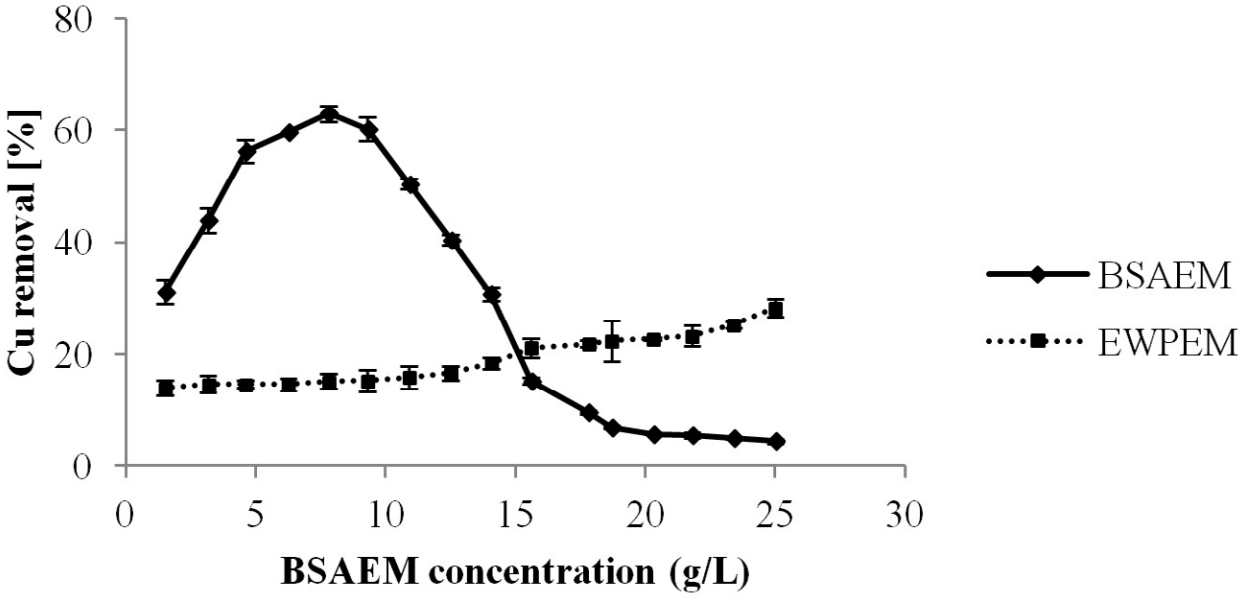

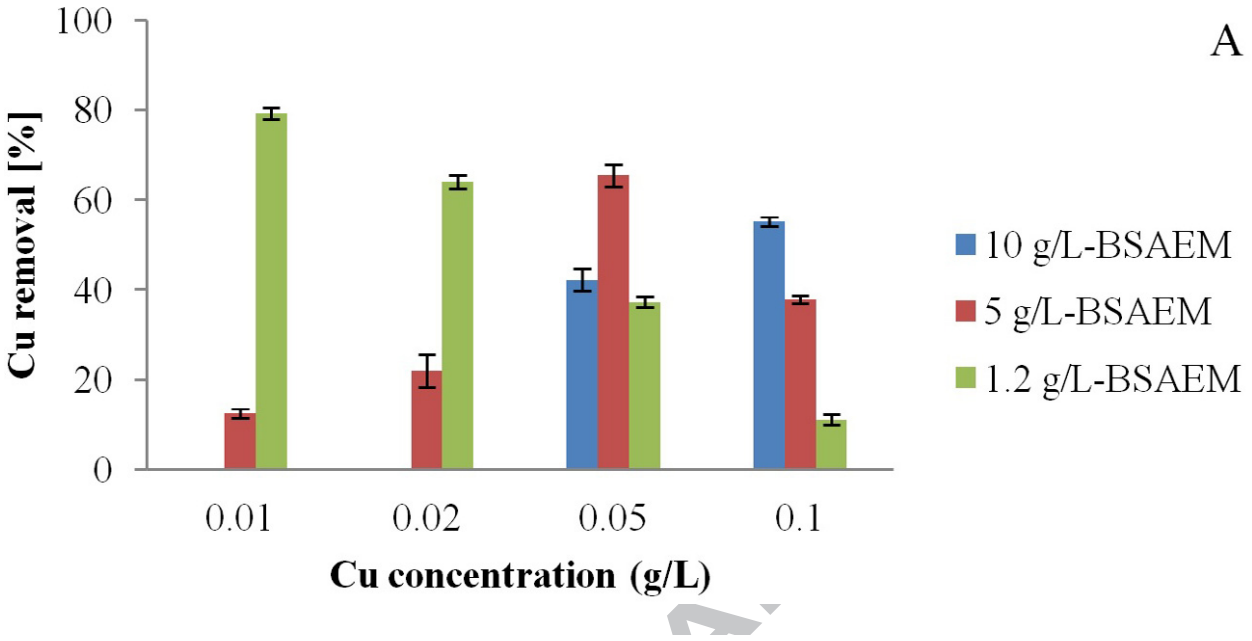
A
100
80
60
40
20
0
Cu removal [%]
0.01
0.02
0.05
0.1
Cu concentration (g/L)
10 g/L-BSAEM
5 g/L-BSAEM
1.2 g/L-BSAEM

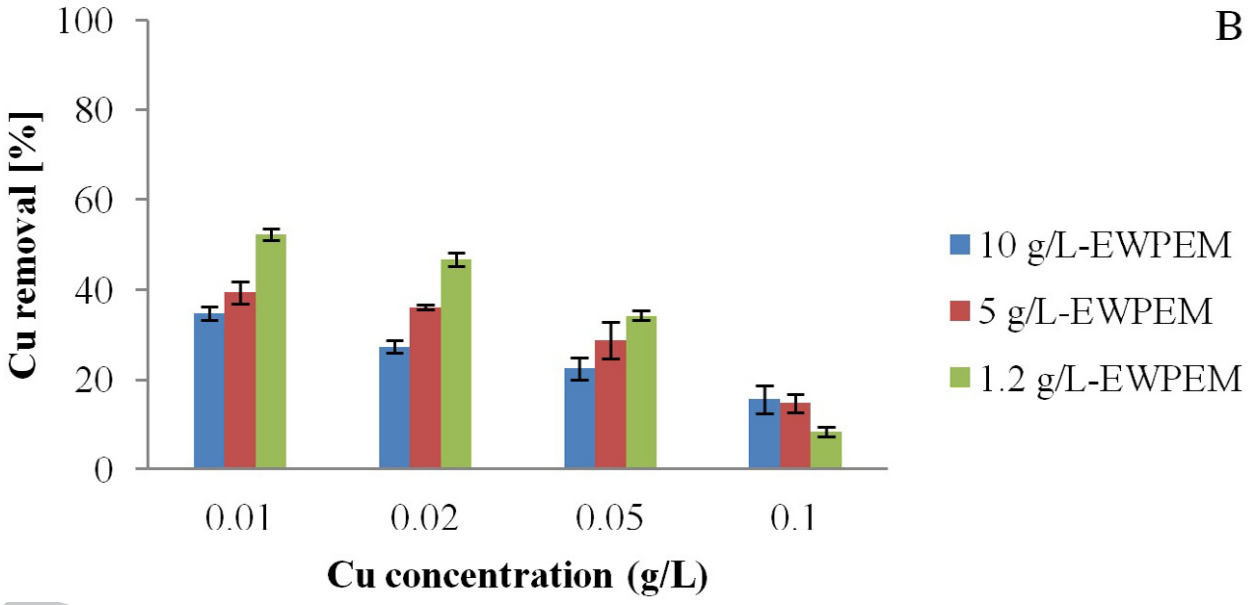
B
100
80
60
40
20
0
Cu removal [%]
0.01
0.02
0.05
0.1
Cu concentration (g/L)
10 g/L-EWPEM
5 g/L-EWPEM
1.2 g/L-EWPEM

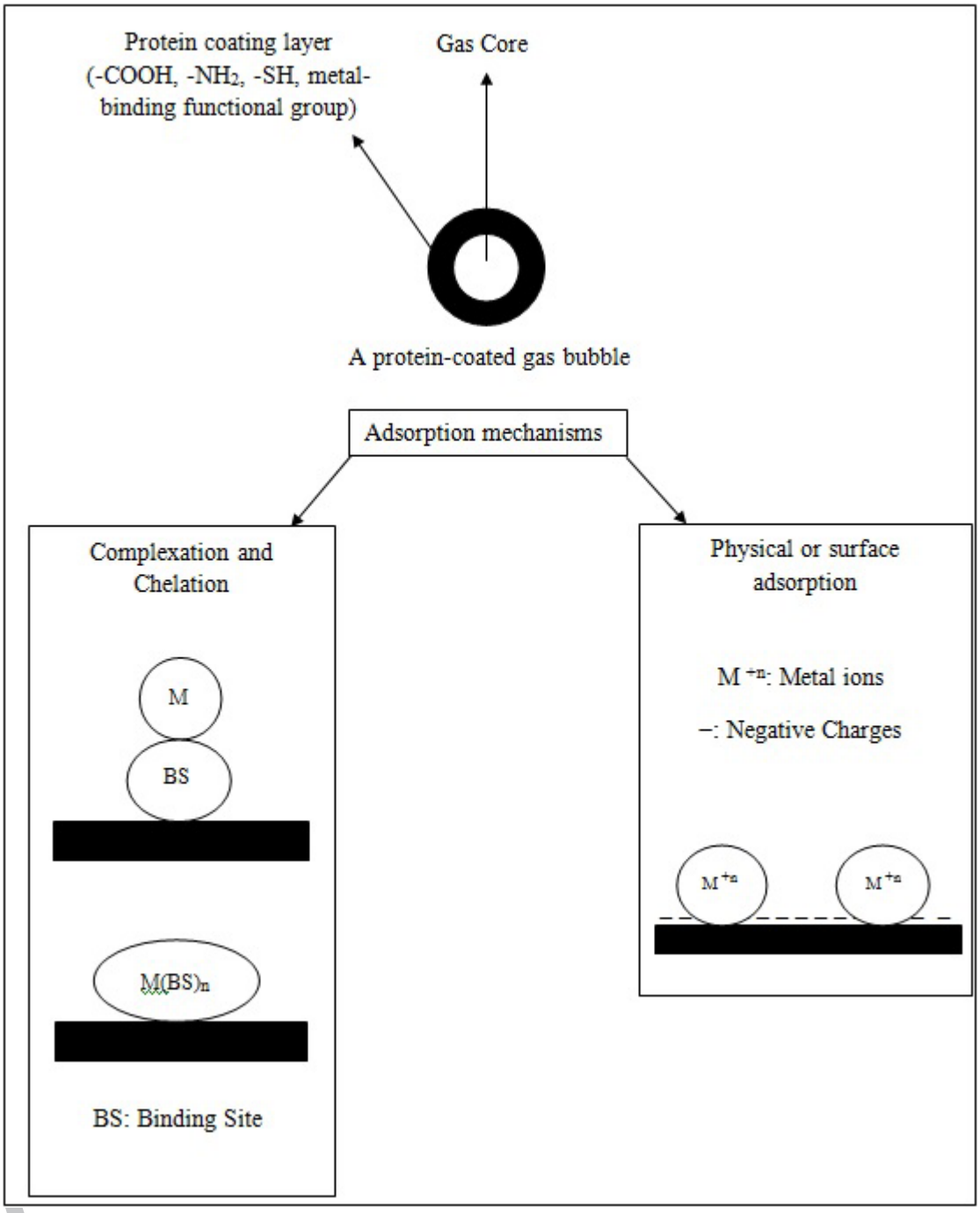

Figure captions:

Figure 1: Schematic view of test setup for emulsion preparation

Figure 2: FTIR spectra of A) BSA and B) EWP before and after copper adsorption

Figure 3: XPS survey scanning spectrum of (A) as received BSA and (B) Cu-loaded BSAEM

Figure 4: XPS survey scanning spectrum of (A) as received EWP and (B) Cu-loaded EWPEM

Figure 5: S2p spectra of (A) BSAEM and (B) EWPEM before and after copper adsorption

Figure 6: Cu2p spectra of (A) Cu-loaded BSAEM and B) Cu-loaded EWPEM

Figure 7: Effect of solution pH on copper removal (Copper concentration: 0.1 g/L, biosorbent concentration: 10 g/L, Contact time: one day, temperature: 20 °C). Each error bar illustrates the standard deviation of five copper concentration measurements.

Figure 8: pH- Zeta potential diagrams of A) BSAEM and B) EWPEM

Figure 9: Effect of temperature on copper removal (Copper concentration: 0.1 g/L, biosorbent concentration: 10 g/L, Contact time: 2 hours, solution pH: 5). Each error bar illustrates the standard deviation of five copper concentration measurements.

Figure 10: Effect of BSAEM and EWPEM dosage on copper removal (Copper concentration: 0.1 g/L, Contact time: one day, solution pH: 5, temperature: 20 °C). Each error bar illustrates the standard deviation of five copper concentration measurements.

Figure 11: Effect of copper concentration on copper removal for A) BSAEM and B) EWPEM (Biomass concentration: 1.2, 5 and 10 g/L, Contact time: one day, solution pH: 5, temperature: 20 °C). Each error bar illustrates the standard deviation of five copper concentration measurements.

Figure 12: Proposed mechanism for copper adsorption by BSAEM and EWPEM.

Table1. Details of batch adsorption experiment.

Parameter	pH	Temperature	C_{Cu}	C_{EM}
pH	1.5-5	20 °C	0.1 g/L	10 g/L
Temperature	5	20 °C-65 °C	0.1 g/L	10 g/L
C_{Cu}	5	20 °C	0.01-0.1 g/L	10 g/L
C_{EM}	5	20 °C	0.1 g/L	1.5-25 g/L

Table 2. Details of acid digestion experiment.

Stage	HCl	HNO_3	H_2O_2	Temperature	Time (h)
1st	5 mL	-----	-----	95 °C	2
2nd	-----	2 mL	0.5 mL	95 °C	1

Table 3. Wave numbers for main band in FTIR.

Functional group	Wave number (cm^{-1})				
	EWP	EWPEM-Cu	BSA	BSAEM-Cu	Ref.
$–NH_2$ stretching	3326	3353	3342	3304	(Pagnanelli et al., 2000)
C–H asymmetric stretching of $–CH_2$	2967	2973	2967	2960	(Wang et al., 2010)
C–H symmetric stretching of $–CH_2$	2876	2881	2875	2875	(Wang et al., 2010)
C O and C–N (amide I) stretching	1695	1700	1692	1694	(Deng and Ting, 2005)
C–N stretching and N–H (amide II) bending	1568	1560	1555	1559	(Sun et al., 2011)
C–H bending	1455	-------	1445	1456	(Bueno et al., 2008)
	1402	-------	1399	1394	(Bueno et al., 2008)
C–N bending	1159	-------	1174	1170	(Deng and Ting, 2005)
C–O bending	1079	-------	-------	-------	(Villaescusa et al., 2004)

Table 4. Binding energies of S and Cu in BSAEM and EWPEM before and after copper adsorption.

Valence state	Sample	Component	Binding energy (eV)
S2p3/2	BSA	S–S	163.5
	Cu-loaded BSAEM	Cu–S	161.5
		S–S	163.5
		S–O	168
	EWP	S–S	163.2
	Cu-loaded EWPEM	Cu–S	161.6
		S–S	163.4
		S–O	167.9
S2p1/2	BSA	S–S	164.7
	Cu-loaded BSAEM	Cu–S	162.8
		S–S	164.7
		S–O	169.3
	EWP	S–S	164.4
	Cu-loaded EWPEM	Cu–S	162.6
		S–S	164.7
		S–O	169.3
Cu2p3/2	Cu-loaded BSAEM	Cu (0), Cu_2O, Cu–S	932.4
		CuO	934.6
	Cu-loaded EWPEM	Cu(0), Cu_2O,Cu–S	932.8
		CuO	934.8
Cu2p1/2	Cu-loaded BSAEM	Cu(0), Cu_2O,Cu–S	952.3
		CuO	954.6
	Cu-loaded EWPEM	Cu(0), Cu_2O, Cu–S	952.6
		CuO	934.5

Table 5. Copper speciation at pH >6 (adapted from Doyle and Liu, 2003).

Species	Reaction
$Cu(OH)^+$	$Cu^{2+} + H_2O \rightleftharpoons Cu(OH)^+ + H^+$
$Cu(OH)_2$	$Cu^{2+} + 2H_2O \rightleftharpoons Cu(OH)_2 + 2H^+$
$Cu(OH)_3^-$	$Cu^{2+} + 3H_2O \rightleftharpoons Cu(OH)_3^- + 3H^+$
$Cu(OH)_4^{2-}$	$Cu^{2+} + 4H_2O \rightleftharpoons Cu(OH)_4^{2-} + 4H^+$

Highlights

- Air-filled emulsions (AFE) generated using egg white protein (EWP) and bovine serum albumen (BSA)
- Proteins removed copper ions from dilute aqueous solutions
- XPS and FTIR showed that the thiol, amino and carboxylic groups were responsible for copper removal
- Temperature and pH played an important role in copper removal